INTERNATIONAL JOURNAL FOR NUMERICAL METHODS IN FLUIDS
*Int. J. Numer. Meth. Fluids* 2010; **63**:297–312
Published online 11 May 2009 in Wiley InterScience (www.interscience.wiley.com). DOI: 10.1002/fld.2067

# High-fidelity aerodynamic shape optimization of modern transport wing using efficient hierarchical parameterization

A. M. Morris, C. B. Allen*, † and T. C. S. Rendall

*University of Bristol, Avon, BS8 1TR, U.K.*

SUMMARY

Aerodynamic shape optimization technology is presented, using an efficient domain element parameterization approach. This provides a method that allows geometries to be parameterized at various levels, ranging from gross three-dimensional planform alterations to detailed local surface changes. Design parameters control the domain element point locations and, through efficient global interpolation functions, deform both the surface geometry and corresponding computational fluid dynamics volume mesh, in a fast, high quality, and robust fashion. This results in total independence from the mesh type (structured or unstructured), and optimization independence from the flow-solver is achieved by obtaining gradient information for an advanced gradient-based optimizer by finite-differences. Hence, the optimization tool can be used in conjunction with any flow-solver and/or mesh generator. Results have been presented recently for two-dimensional aerofoil cases, and shown impressive results; drag reductions of up to 45% were demonstrated using only 22 active design parameters. This paper presents the extension of these methods to three dimensions, with results for highly constrained optimization of a modern aircraft wing in transonic cruise. The optimization uses combined global and local parameters, giving 388 design variables, and produces a shock-free geometry with an 18% reduction in drag, with the added advantage of significantly reduced root moments. Copyright © 2009 John Wiley & Sons, Ltd.

Received 20 June 2008; Revised 20 March 2009; Accepted 23 March 2009

KEY WORDS: CFD; shape parameterization; mesh deformation; radial basis functions; aerodynamics; numerical optimization; drag minimization

## 1. INTRODUCTION

Computational fluid dynamics (CFD) methods are now commonplace in aerospace industries and at the forefront of analysis capabilities, providing a fast and effective method of predicting a design's

*Correspondence to: C. B. Allen, University of Bristol, Avon, BS8 1TR, U.K.
†E-mail: c.b.allen@bristol.ac.uk, c.b.allen@bris.ac.uk

aerodynamic performance. However, with the increasing complexity of designs, engineers often struggle to interpret the intricacies of the CFD results sufficiently to be able to manually alter the geometry to improve performance. Hence, there has been an increase in demand for intelligent and automatic shape optimization schemes. This requires combining geometry control methods with numerical optimization algorithms, to provide a mechanism to mathematically seek improved and optimum designs, using CFD as the analysis tool.

Shape optimization requires consideration of three issues, each of which have numerous solutions: shape parameterization including CFD surface and volume mesh deformation, computation of the design variable derivatives, and effective use of these derivatives to improve design. Geometry parameterization is critical for effective shape optimization, and is the method of representing the design surface, and defining the degrees of freedom in which the geometry can be altered and, ideally, this should be linked with an effective method of deforming the design surface and volume mesh in a corresponding fashion. Parameterizing complex shapes remains a serious obstacle to both the manual and automatic CFD-based optimizations, and a wide variety of shape control and morphing methods have been developed, see for example [1–11]. However, many of these approaches do not allow sufficiently free-form design and can produce infeasible shapes [12, 13]. Furthermore, most methods do not have a suitable method to deform the CFD mesh once the surface has been changed, and regeneration is often required. This may not be a problem for simple geometries, small geometric changes, and/or small meshes, but can in some cases make automation of the optimization process impossible.

Exploration of as much of the design space as possible is important, but having an excessive number of deformation degrees of freedom (design variables) can make optimization impractically expensive. Hence, an efficient domain element shape parameterization technique has been developed, wherein design surface and volume mesh deformation are accomplished through global interpolations using radial basis functions (RBFs), such that when the positions of the domain element are altered, both the design surface and its corresponding CFD volume mesh are deformed in a high-quality fashion [14, 15]. The parameterization technique allows for geometry control at various fidelity levels, ranging from fine, detailed surface geometry changes to gross three-dimensional planform alterations. Furthermore, the method works on point clouds, i.e. no connectivity information is required, and so is totally independent of the CFD mesh type, removing any mesh generation or flow-solver dependence.

Independence from the flow-solver is ensured by obtaining the sensitivities required for optimization via finite-difference. This allows numerous options in terms of optimization approaches, and an advanced feasible sequential quadratic programming (FSQP) [16–18] gradient-based optimizer has been integrated into the framework. Independence from both mesh generation approach and flow-solver ensures a totally generic tool has been developed. This advanced optimization based on domain element parameterization has been proven in two dimensions, demonstrating large drag reductions for highly constrained aerofoil cases, both viscous and inviscid [19, 20].

Hence, this paper presents the extension to three dimensions of the shape parameterization, mesh deformation, and optimization method. Optimization is applied here to the Multidisciplinary Optimization (MDO) wing (a large modern transport aircraft wing, the result of a previous European Community (EC) project [21–23]) in the transonic cruise condition. Detailed results of the optimization performed with the highest fidelity so far used are presented. This is a combination of global parameters and local surface geometry changes, resulting in 388 design variables, and the objective is drag minimization.



DOI: 10.1002/fld

## 2. DOMAIN ELEMENT PARAMETERIZATION

Finite-differences are used here to compute design variable sensitivities, since a 'wrap-around' framework has been developed. Hence, the choice of parameterization method is absolutely critical in terms of the computational cost of any optimization and an efficient method, i.e. as few design variables as possible, is essential. However, the method must still allow sufficient free-form design such that any likely optimum design that may exist is achievable.

Numerous parameterization methods have been presented for CFD shape optimization, and these can be split into those that parameterize the aerodynamic mesh or those that parameterize the design geometry from which a mesh is generated. Mesh parameterization methods are generally independent of the mesh generation package. This requires a mesh deformation algorithm, but allows the use of previously generated meshes for optimization. Methods of this nature include discrete [24–26], analytical, basis vector [4], free-form deformation (FFD) [5], and domain element methods [27]. Geometry parameterization methods are inherently linked with the mesh generation package, and optimization requires automatic mesh generation tools. Methods of this nature include partial differential equation methods [1, 8], polynomial or spline [9], CAD, and recently CST [10, 11] methods. The reader is referred to [28, 29] for comprehensive reviews of parameterization methods.

The parameterization method developed here uses a domain element to control the shape of the design surface. A global multivariate interpolation has been developed using RBFs, which then controls the surface geometry and the locations of the volume mesh points directly from the domain element node locations. All points are treated as point clouds, so the parameterization technique is totally independent from the mesh type and generation package. The mapping is only required once for the initial design, and updates to the geometry and the corresponding mesh are provided simultaneously by application of the multivariate interpolation; this is extremely fast and efficient. In [15] it was demonstrated that the initial mesh quality is preserved, even for large surface deformations, for the same MDO geometry considered here.

The three-dimensional domain element consists of an evenly distributed series of two-dimensional slices located according to local surface geometry. However, individual locations of the domain element points are not chosen as the design variables, but a hierarchy of intuitive shape deformation design variables has been developed. So far, three levels of design variables have been adopted. At the most global level, design variables correspond to motions of all domain element nodes simultaneously, for example altering wing angle of attack, sweep, or twist. At the intermediate level, design variables control the rotation, chord, thickness, and position of each two-dimensional domain element slice separately, and at the most local level very small groups or individual domain element nodes are altered to provide detailed and local shape changes.

An example parameterization and deformation of a cylinder surface is presented in Figure 1. Figure 1(a) shows the original surface and domain element; seven square domain element slices are used, and examples of local, intermediate, and global deformations are shown. (b) shows movement of an individual domain element point, a local design variable, (c) shows the rigid twist of the fourth slice, an intermediate design variable, and (d) shows rigid linear twist of the entire domain element, a global design variable. Also shown in (e) is a combination of global twist and a local perturbation. The interpolation method is seen to provide a smooth surface change, and smooth and very high-quality mesh deformation results from this, see [15]. Figure 2 depicts the domain element parameterization of the MDO wing considered in this paper.



DOI: 10.1002/fld

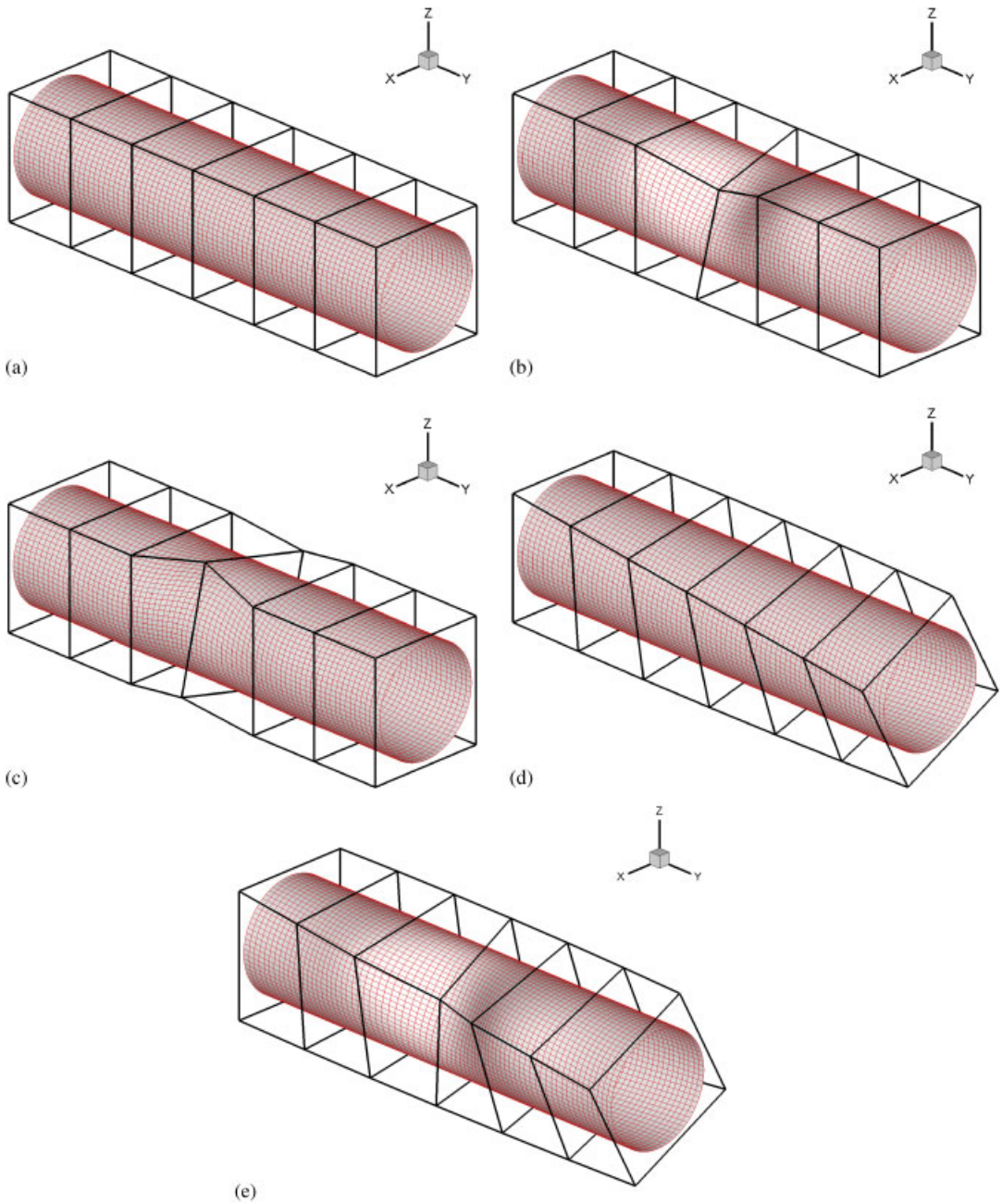


Figure 1. Cylinder parameterization example: (a) cylinder surface and domain element; (b) local perturbation; (c) intermediate perturbation; (d) global perturbation; and (e) combined local and global perturbation.



DOI: 10.1002/fld

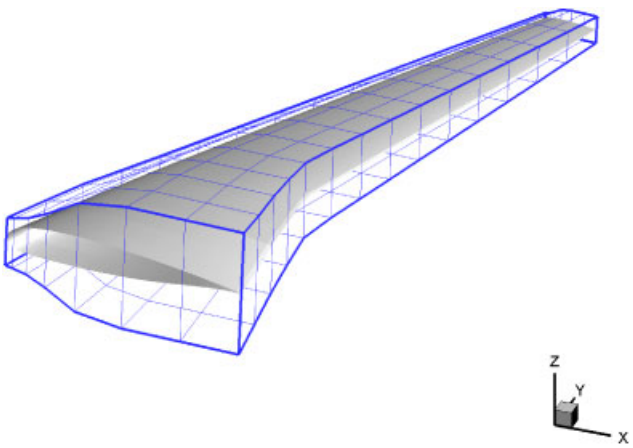


Figure 2. MDO parameterization.

### 2.1. *Parameterization formulation*

The global dependence between the domain element nodes and the aerodynamic mesh points can be evaluated, using RBFs [30, 31], and this transfers a deformation of the element, due to a design variable change, to smoothly alter the aerodynamic shape and its corresponding CFD volume mesh. Using this method, only an initial mesh of the original design is required to allow optimization. The interpolation method developed here requires no connectivity information, and can therefore be applied equally well to either structured and unstructured mesh topologies. Domain element points and volume mesh points are simply treated as independent point clouds with the dependence matrix computed only once.

The method used here is similar to that detailed in Allen and Rendall [14, 15], where it is applied to both CFD–CSD coupling and mesh deformation. The solution of an interpolation problem using RBFs begins with the form of the required interpolation

$$f(\mathbf{x}) = \sum_{i=1}^{i=N} \gamma_i \phi(\|\mathbf{x} - \mathbf{x_i}\|) \tag{1}$$

where $f(\mathbf{x})$ is the function approximated, the index $i$ identifies the centres for the interpolation (the domain element nodes in this case), $\mathbf{x_i}$ is the location of that centre, and $\phi$ is the function used. A polynomial term can also be added, to ensure certain properties of the interpolation, see [14, 15], but is not required here. The coefficients $\gamma_i$ are then found by requiring exact recovery of the original control points.

A system needs to solved relating to the domain element nodes, to evaluate the coefficients associated with them. Exact recovery of the centres gives (subscript $d$ represents a domain element control point)

$$\mathbf{x}_d = \mathbf{C}\ \mathbf{a}_x \tag{2}$$

$$\mathbf{y}_d = \mathbf{C}\ \mathbf{a}_y \tag{3}$$

$$\mathbf{z}_d = \mathbf{C}\ \mathbf{a}_z \tag{4}$$



DOI: 10.1002/fld

where

$$\mathbf{x}_d = \begin{pmatrix} x_{d_1} \\ \vdots \\ x_{d_N} \end{pmatrix}, \quad \mathbf{a}_x = \begin{pmatrix} \gamma_1^x \\ \vdots \\ \gamma_N^x \end{pmatrix} \tag{5}$$

(Analogous definitions hold for $\mathbf{y}_d$ and $\mathbf{z}_d$ and their $\mathbf{a}$ vectors) and

$$\mathbf{C} = \begin{pmatrix} \phi_{d_1 d_1} & \phi_{d_1 d_2} & \cdots & \phi_{d_1 d_N} \\ \vdots & \vdots & \ddots & \vdots \\ \phi_{d_N d_1} & \phi_{d_N d_2} & \cdots & \phi_{d_N d_N} \end{pmatrix} \tag{6}$$

where $N$ is the number of domain element nodes. In the above

$$\phi_{d_1 d_2} = \phi(\|\mathbf{x}_{d_1} - \mathbf{x}_{d_2}\|) \tag{7}$$

indicates the basis function evaluated on the distance between $d_1$ and $d_2$. To locate the aerodynamic mesh point positions resulting from the domain element positions, the following matrix must be formed, where subscript $a$ indicates an aerodynamic node:

$$\mathbf{A} = \begin{pmatrix} \phi_{a_1 d_1} & \phi_{a_1 d_2} & \cdots & \phi_{a_1 d_N} \\ \vdots & \vdots & \ddots & \vdots \\ \phi_{a_M d_1} & \phi_{a_M d_2} & \cdots & \phi_{a_M d_N} \end{pmatrix} \tag{8}$$

where $M$ is the number of aerodynamic mesh points. The positions of the aerodynamic mesh points, given by the vectors $\mathbf{x}_a$, $\mathbf{y}_a$, and $\mathbf{z}_a$, can then be computed by

$$\mathbf{x}_a = \mathbf{A}\ \mathbf{a}_x = \mathbf{A}\ \mathbf{C}^{-1}\mathbf{x}_d = \mathbf{H}\mathbf{x}_d \tag{9}$$

$$\mathbf{y}_a = \mathbf{A}\ \mathbf{a}_y = \mathbf{A}\ \mathbf{C}^{-1}\mathbf{y}_d = \mathbf{H}\mathbf{y}_d \tag{10}$$

$$\mathbf{z}_a = \mathbf{A}\ \mathbf{a}_z = \mathbf{A}\ \mathbf{C}^{-1}\mathbf{z}_d = \mathbf{H}\mathbf{z}_d \tag{11}$$

There are many ways to implement this approach, but these are not considered here. The parameterization and RBF interpolation methods have several key properties:

- The number of design variables required to allow free-form design can be very low when compared with other methods [20].
- Design variables can range in fidelity from the coordinate of a single domain element location, providing a detailed surface geometry change, to a gross three-dimensional deformation such as sweep distribution. This can allow designers to choose the fidelity of the optimization.
- Global parameters, for example angle of attack or wing sweep, can be included as design variables. This is impossible in many other optimization approaches, wherein these quantities have to be adjusted externally to attempt to satisfy constraints.
- The parameterization technique is independent of the initial geometry, with the domain element positioned automatically according to the solid surface. This can allow very complex or multi-element geometries to be parameterized.



DOI: 10.1002/fld

- The interpolation is independent of mesh type or structure, as the position vectors are simply mesh positions in any order.
- The interpolation is time-invariant, and so only needs to be computed once, prior to any simulation. The surface geometry and mesh are then deformed very efficiently by matrix–vector multiplication.
- The interpolation is perfectly parallel, as the matrix and the position vectors can simply be split into rows and elements required for each partition.

Domain element methods work well with RBF mesh deformation due to the low number of domain element node points. However, if one were to use spline control points or surface mesh points in three dimensions, then computational memory issues must be considered [32], but these are not considered here.

## 3. OPTIMIZATION METHOD

There are numerous possible approaches in terms of optimization, but practical optimization of aerodynamic performance of a solid body requires the capability of imposing constraints, for example minimum thickness, minimum volume, minimum lift, maximum moment, etc. Constrained gradient-based optimizers are fast and efficient at providing solutions to local optimization problems [18, 33], and unconstrained optimizers can incorporate constraints by using a penalty function for designs that are near or beyond the constraint boundary, but these methods are now considered inefficient and have been replaced by methods that focus on the solution of the Kuhn–Tucker equations.

The solution of these equations forms the basis of the nonlinear programming algorithm used here. A constrained quasi-Newton method guarantees superlinear convergence by accumulating second-order information relating to the Kuhn–Tucker equations using a quasi-Newton updating procedure; i.e. at each major iteration, an approximation is made of the Hessian of the Lagrangian function. This is then used to generate a quadratic programming (QP) subproblem where the solution is used to form a search direction for a line search procedure. This forms the basis of a sequential quadratic programming (SQP) algorithm, and this approach has been shown to outperform other tested methods in terms of efficiency, accuracy, and percentage of successful solutions, over a number of test problems [34]. An FSQP algorithm is used in the current research and this was originally developed in [16–18]. This particular algorithm has been implemented across a wide range of optimization problems, most relevant to the application here is the work of Qin and coworkers [35–38] where the algorithm was used for CFD-based-constrained optimization of a blended wing body using an inviscid adjoint solver to obtain the sensitivities. The sensitivities are obtained here via finite-differences, since a generic optimization tool, independent of the flow-solver used, is the ultimate objective of this work. To ensure no biasing towards one direction and to increase accuracy, a second-order accurate central-difference finite-difference stencil is used.

## 4. THREE-DIMENSIONAL AERODYNAMIC OPTIMIZATION

The MDO wing corresponds to a typical design of a large modern transport aircraft wing, with its primary design point being that of transonic cruise flight efficiency. At this design point the objective of optimization is minimum drag, but this must be achieved without detriment to other aerodynamic,



DOI: 10.1002/fld

structural, and geometric quantities. Hence, four strict constraints were imposed, to ensure that improvements achieved can be attributed solely to improvements in the geometric design.

1. Total lift $\geqslant$ total lift of initial wing. This is an essential constraint, and involves total lift and not lift coefficient.
2. Root bending moment $\leqslant$ root bending moment of the initial wing. Major structural members of the wing are sized according to these loads, and as such any increased moment would impact negatively on wing structural weight.
3. Root torsion moment $\leqslant$ root torsion moment of the initial wing, imposed for the same reasons as given in the above constraint.
4. Internal volume $\geqslant$ internal volume of initial wing. It has been demonstrated in previous works [20] that reductions in drag can be achieved by allowing internal volume to decrease, and so these designs do not truly represent design improvements.

The economical cruise flight Mach number for the MDO wing defined by Allwright [21–23] is 0.85, with the wing trimmed to obtain a lift coefficient of 0.452. This design case is well suited to inviscid flow analysis by solution of the Euler equations, since induced and wave drag form a major part of the total drag. Furthermore, two-dimensional aerofoil optimizations have shown previously that the improvements achieved through inviscid optimizations in transonic Mach numbers are also realized in viscous analysis [19, 20]. A 330 000 point-structured multiblock mesh was used, generated by the techniques of Allen [39]. Flow solutions are provided by an inviscid, structured multiblock finite volume upwind solver [40–43] using the flux vector splitting of van Leer [44, 45] and incorporating multigrid acceleration [46].

### *4.1. Results*

The optimization was run with the following design parameters:

1. *Global*: Only two issues are considered, dihedral and sweep. There are 15 domain element slices, and the root section is fixed in position and, hence, there are 14 sweep design variables and 14 dihedral variables (28 parameters).
2. *Intermediate*: Each domain element slice has three local design variables, the $(x, z)$ location of the quarter chord point and the rotation of that element (45 parameters).
3. *Detailed*: Each two-dimensional domain element slice also has the full set of 21 active design variables developed for free-form aerofoil design [19, 20] (315 parameters).

The three levels of parameters above are combined to give a total of 388 active design variables. It should be noted that if level 1 parameterization was used alone, wing angle of attack and a twist parameter would need to be added, and level 2 parameterization alone would also include chord and thickness for each domain element, but these are already included in the parameters in level 3, so are not required when combined.

The results of this optimization are given in Table I. Hence, free-form control of aerofoil profile geometries combined with design variables that enable truly three-dimensional planform alterations here achieves a reduction in drag coefficient of over 18%, and this is a significant reduction. Along with the objective and constraint parameters, the table also shows the volume entropy value. The local value of entropy in each cell is evaluated using Equation (12) and the total value in the entire domain is summed using (13). This represents a measure of the amount of non-isentropic processes in the entire flow field. The reduction achieved here is due to the reduction of shock



DOI: 10.1002/fld

Table I. Wing optimization results.

| | Initial | Optimized | %Diff |
|---|---|---|---|
| Cl | 0.4523 | 0.4530 | +0.14 |
| $Cm_{bending}$ | 0.1340 | 0.1004 | −25.03 |
| $Cm_{torsion}$ | −0.0547 | −0.0471 | −13.93 |
| Volume | 387.14 | 401.60 | +3.73 |
| **Cd** | 0.02780 | 0.02287 | **−18.29** |
| Entropy | 0.0149 | 0.0123 | −16.91 |

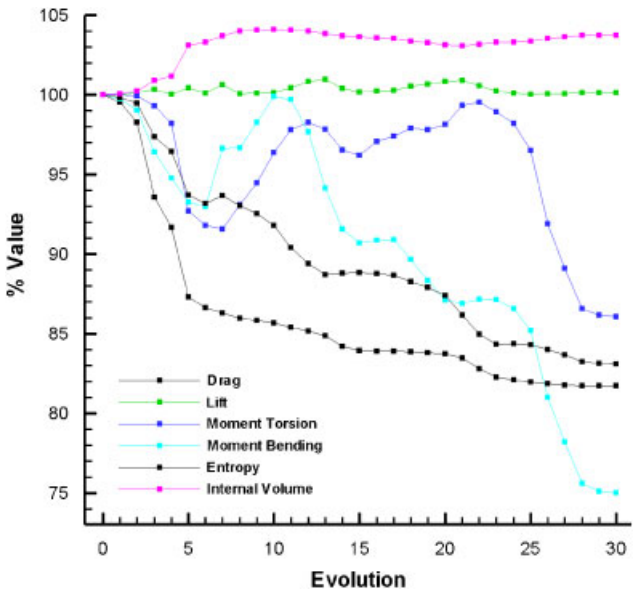


Figure 3. Optimization history.

strength, and clearly highlights the link between entropy and drag generation. It was also shown in [19, 20] that field entropy is an interesting quantity to examine and may even be a useful objective function.

$$e = \frac{P_{\text{local}}/\rho_{\text{local}}^{\gamma}}{P_{\infty}/\rho_{\infty}^{\gamma}} - 1 \tag{12}$$

$$e_{\text{vol}} = \frac{\sum_{N=1}^{\text{Ncells}} e_N * V_N}{\sum_{N=1}^{\text{Ncells}} V_N} \quad \text{where } V_N \text{ is cell volume} \tag{13}$$

Figure 3 shows the optimization history of objective function and constraints, showing that only 30 evolutions are required (in fact 40 evolutions were performed but there were no changes after 29). Optimization has had the beneficial effect of significantly reducing both root bending and root torsion moments. In addition wing internal volume has increased slightly.



DOI: 10.1002/fld

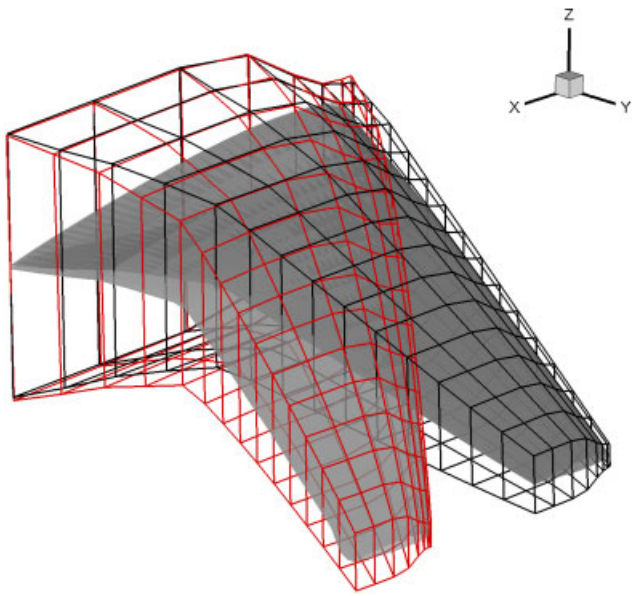


Figure 4. MDO parameterization: MDO wing and domain element.

Initial and optimized domain element and wing geometries are depicted in Figures 4 and 5. The most notable change to the optimized wing is to the sweep distribution; not only has sweep been increased significantly, but the leading edge is no longer straight such that there is increased sweep angle towards the tip. Root torsion moment is rigidly constrained and an increased sweep angle normally impacts negatively on this, but observation of Figure 8 demonstrates that loading has moved significantly inboard such that sweep angle can be increased in an effort to reduce drag with no penalty to root torsion moment. In fact both root torsion and root bending moments have been reduced significantly when compared with the initial MDO wing, and reduced root moments could provide possible weight savings. Figure 8 also shows that drag has increased slightly inboard due to the increased loading there, but at all outboard locations the drag is significantly reduced.

The optimized wing has been deformed considerably from its initial geometry. Figure 6 depicts views of CFD surface and volume meshes corresponding to initial and optimized wing geometries. Even though the deformation is dramatic, the parameterization method preserves a high-quality CFD mesh.

Figure 7 depicts contours of coefficient of pressure ($C$p) for the initial MDO and optimized wing geometries, showing the large change in flow structure. Figure 9 also shows the sectional $C$p distributions of the initial MDO and optimized wings, transformed on to a rectangular wing of unit chord and span to enable comparison.

The MDO wing in its economical cruise flight exhibits a strong shock along the entire length of the span. The free-form design control allowable by the parameterization developed here achieves a reduction in drag of over 18% and results in a completely shock-free wing. This is a considerable result considering the constraint on a high value of lift and at a high transonic Mach number. From Figure 9 it is clear that the wing has truly achieved an improvement in geometric design; a smooth $C$p distribution that is completely shock-free along the entire span of the wing is obtained.



DOI: 10.1002/fld

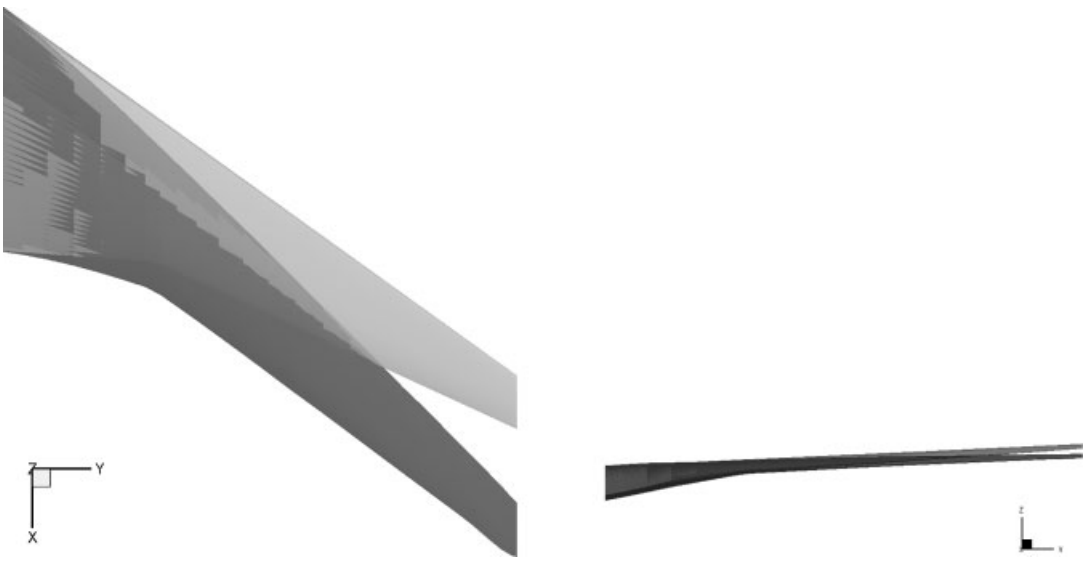


Figure 5. Domain element and wing geometries (initial MDO—light, optimized—dark).

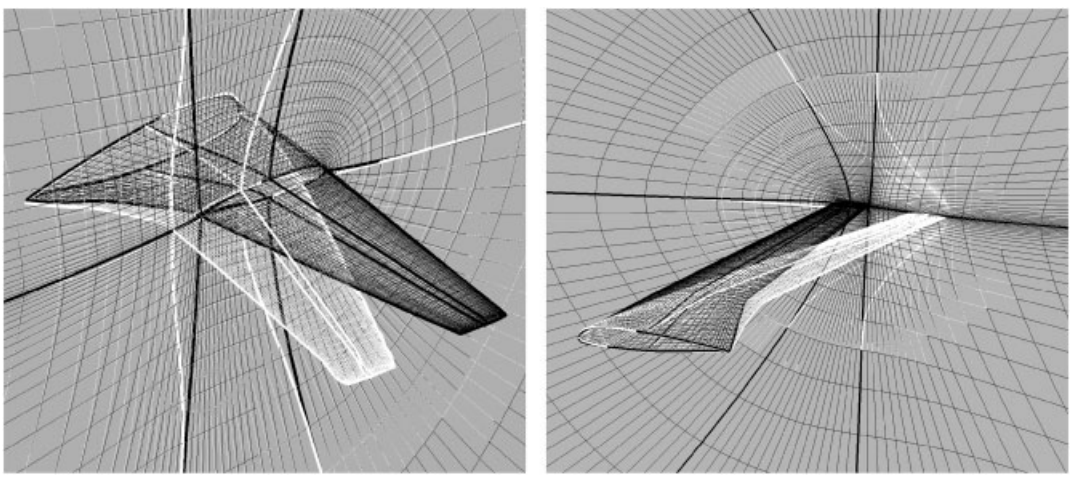

Figure 6. CFD volume mesh deformation. Initial MDO mesh—black, optimized mesh—white.

Sectional slices through the transformed wing are shown in Figure 10 and compared with the initial MDO wing geometry. Significant aerofoil section changes (and twist distribution) are clearly seen. Root incidence is increased, but with a larger wash-out, highlighting that inboard sections are more highly loaded with relief towards the tip. The global smooth interpolation functions used here guarantee that smooth surface changes are applied, and so this approach is equally valid for optimization including viscous effects. However, it should be noted that the results may be slightly different, for example the high suction on the upper surface produced towards the tip would not be



DOI: 10.1002/fld

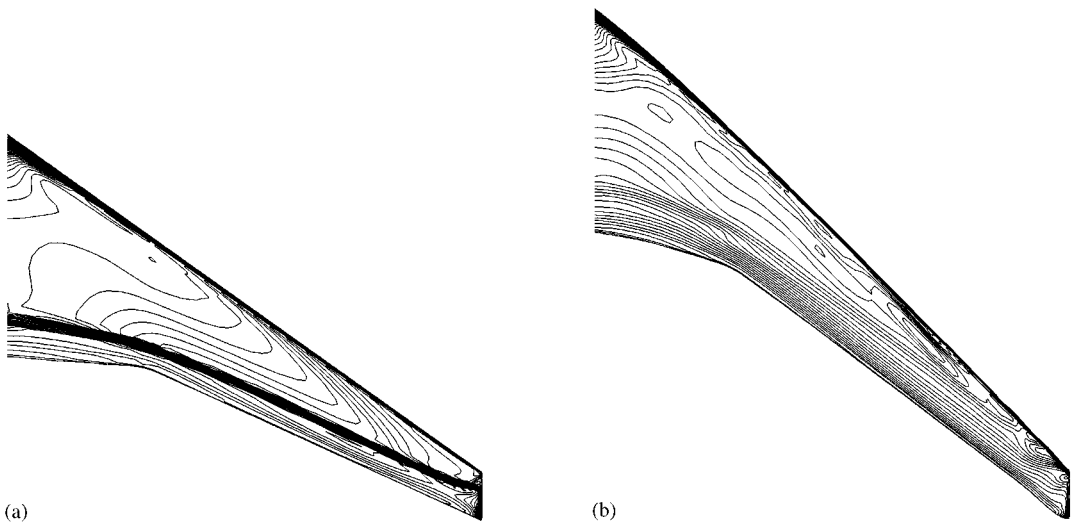


Figure 7. Cp distributions: (a) initial MDO and (b) optimized.

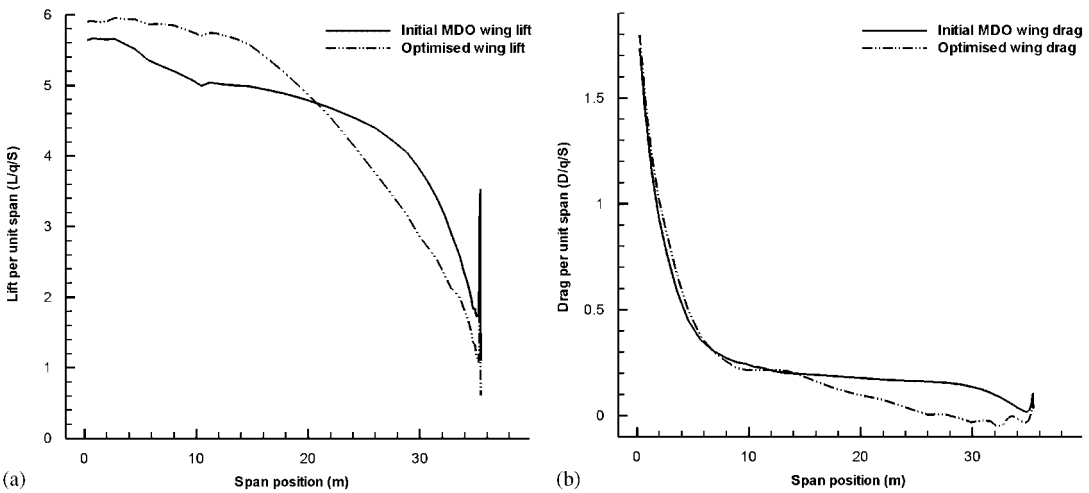


Figure 8. Spanwise distributions: (a) lift and (b) drag.

present in a viscous flow optimization, but the ability to produce subtle surface changes capable of reducing the transonic effects has been proven here.

*4.1.1. Cost.* The cost of the scheme scales almost linearly with the number of design parameters. Each evolution requires a flow solution for two perturbations in each design variable (one positive and one negative to produce a central difference) and an average of around two flow solutions to evaluate the allowable step-size in surface evolution. Hence, this solution required around



DOI: 10.1002/fld

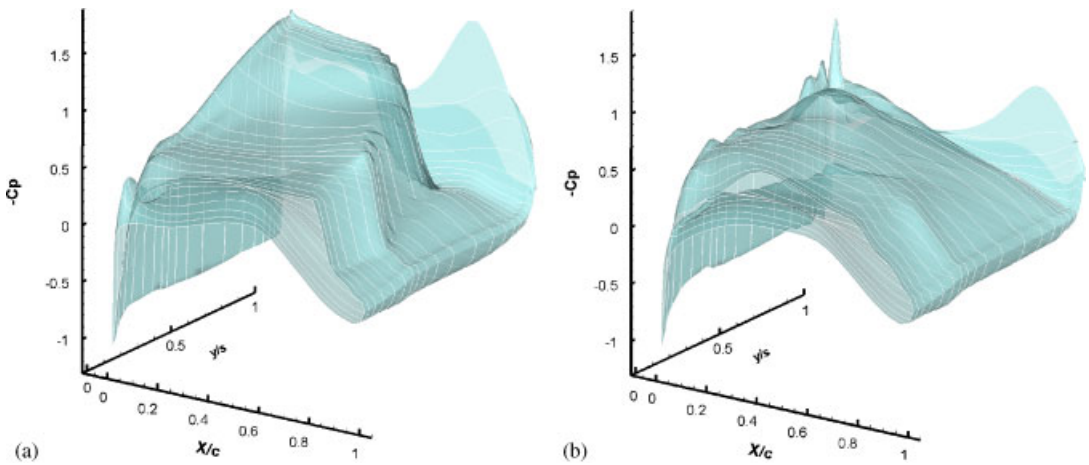


Figure 9. Surface Cp distributions: (a) initial MDO and (b) optimized.

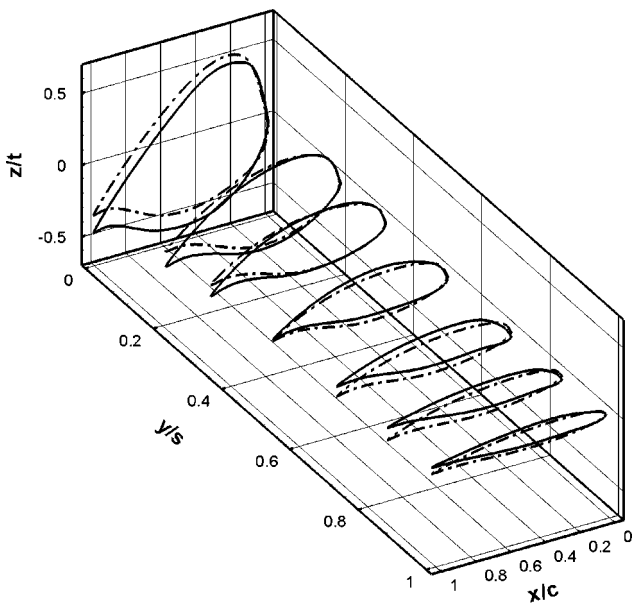


Figure 10. Aerofoil profiles, initial (dashed) and optimized (solid).

23 000 flow solutions for 30 evolutions. However, the method has been parallelized such that each sensitivity evaluation can be performed independently. Each flow solution is also restarted from a previous solution, to significantly reduce the cost.



DOI: 10.1002/fld

## 5. CONCLUSIONS

Aerodynamic shape optimization technology using an efficient domain element parameterization approach has been presented. Design parameters control the domain element point locations and, through efficient global interpolation functions, deform both the surface geometry and corresponding CFD volume mesh, in a fast, high quality, and robust fashion. This domain element technique is mesh topology and mesh generation package independent, requiring only an initial mesh.

The parameterization technique allows the combination of variables of different scales and types with only a few parameterization nodes, and this leads to a significantly reduced number of design variables for three-dimensional applications when compared with many other types of shape parameterization method. Derivatives of these design parameters are computed via second-order finite-differences, to ensure flow-solver independence, and fed into an FSQP gradient-based optimizer.

The optimization tools have been applied to aerodynamic shape optimization of the MDO wing in transonic cruise, with the objective function being drag, subject to strict constraints. Using 388 combined global and local parameters results in a totally shock-free wing with over 18% reduction in inviscid drag, combined with significantly reduced root aerodynamic moments.

Off-design performance has not been considered here, as proof of the optimization method's capability is the primary aim of this paper, but future work will include multi-point optimization using either several objective functions or combining those at different cases, as in [47, 48].

In-house CFD mesh generation and flow solution codes are used here, but the method is completely generic and can be wrapped around any appropriate tools. Furthermore, although an external aerodynamic design problem is presented, this is not a restriction and the methods can be applied to any steady-state fluid dynamic design problem.

ACKNOWLEDGEMENTS

The authors would like to thank: Agusta-Westland, EPSRC (the U.K. Engineering and Physical Sciences Council), and the U.K. MoD Joint Grant Scheme (JGS) funding, under contract GR/S61294 for the part funding of this research and the support of Asa Morris, and the University of Bristol, with whom Thomas Rendall has been awarded a postgraduate research scholarship.

REFERENCES

1. Bloor MIG, Wilson MJ. Efficient parameterization of generic aircraft geometry. *Journal of Aircraft* 1995; **32**(6):1269–1275.
2. DYoung DP, Huffman WP, Melvin RG, Bieterman MB, Hilmes CL, Johnson FT. Inexactness and global convergence in design optimization. *A/AA Paper 94-4286. Fifth AIAA/USAF/NASA/ISSMO Symposium on Multdisciplinary Analysis and Optimization*, Panama City, FL, September 1994.
3. Sobieczky H. In *Parametric Airfoils and Wings*, Fuji K, Dulikravich (eds). Notes on Numerical Fluid Mechanics, vol. 68. Wiesbaden: Vieweg, 1998; 71–88.
4. Pickett RM, Rubinstein MF, Nelson RB. Automated structural synthesis using a reduced number of design coordinates. *AIAA Journal* 1973; **11**(4):494–498.
5. Watt A, Watt M. *Advanced Animation and Rendering Techniques*, Chapter 17. Addison-Wesley: New York, 1992.
6. Hicks RM, Henne PA. Wing design by numerical optimization. *Journal of Aircraft* 1978; **15**:407–412.
7. Hicks RM, Murman EM, Vanderplaats GN. An assessment of aerofoil design by numerical optimization. *NASA TMX-3092*, Ames Research Center, Moffett Field, CA, July 1974.
8. Smith RE, Bloor MIG, Wilson MJ, Thomas T. Rapid airplane parametric input design (RAPID). *Proceedings of 12th AIAA Computational Fluid Dynamics Conference*. AIAA: Washington, DC, 1995; 452–462.



DOI: 10.1002/fld

9. Braibant V, Fleury C. Shape optimal design using B-splines. *Computer Methods in Applied Mechanics and Engineering* 1984; **44**(3):247–267.
10. Kulfan BM, Bussoletti JE. Fundamental parametric geometry representations for aircraft component shapes. *AIAA-2006-6948*, *Eleventh AIAA/ISSMO Multidisciplinary Analysis and Optimization Conference*, 6–8 September 2006.
11. Kulfan BM. A universal parametric geometry representation method—CST. *Forty-fifth AIAA Aerospace Sciences Meeting and Exhibit*, Reno, Nevada, 8–11 January 2007.
12. Castonguay P, Nadarajah SK. Effect of shape parameterization on aerodynamic shape optimization. *Forty-fifth AIAA Aerospace Sciences Meeting and Exhibit*, Reno, Nevada, 8–11 January 2007.
13. Nadarajah S, Castonguay P, Mousavi A. Survey of shape parameterization techniques and its effect on three-dimensional aerodynamic shape optimization. *AIAA-2007-3837*, *Eighteenth AIAA Computational Fluid Dynamics Conference*, Miami, FL, 25–28 June 2007.
14. Allen CB, Rendall TCS. Unified CFD–CSD interpolation and mesh motion using radial basis functions. *AIAA-2007-3804*, *Twenty-fifth AIAA Alied Aerodynamics Conference*, Miami, June 2007.
15. Rendall TCS, Allen CB. Unified fluid–structure interpolation and mesh motion using radial basis functions. *International Journal for Numerical Methods in Engineering* 2008; **74**(10):1519–1559.
16. Zhou JL, Tits AL, Lawrence CT. User's guide for FFSQP version 3.7: a Fortran code for solving optimization programs, possibly minimax, with general inequality constraints and linear equality constraints, generating feasible iterates. *Technical Report SRC-TR-92-107r5*, Institute for Systems Research, University of Maryland, College Park, 1997.
17. Zhou JL, Tits AL. Nonotone line search for minimax problems. *Journal of Optimization Theory and Applications* 1993; **76**(3):455–476.
18. Panier E, Tits AL. On combining feasibility, descent and superlinear convergence in inequality constrained optimization. *Mathematical Programming* 1993; **59**:261–276.
19. Morris AM, Allen CB, Rendall TCS. Development of generic CFD-based aerodynamic optimization tools for helicopter rotor blades. *AIAA-2007-3809*, *Twenty-fifth AIAA Alied Aerodynamics Conference*, Miami, FL, June 2007.
20. Morris AM, Allen CB, Rendall TCS. CFD-based optimization of aerofoils using radial basis functions for domain element parameterization and mesh deformation international. *International Journal for Numerical Methods in Fluids* 2008; **58**(8):827–860.
21. Allwright S. Multi-discipline optimization in preliminary design of commercial transport aircraft. *ECCOMAS*, Computational Methods in Allied Sciences. Wiley: New York, 1996; 523–526.
22. Allwright S. Reference aircraft performance and primary sensitivities. *Technical Report D.3.12.R*, *MDO/TR/BAE/SA970530/1*.
23. Haase D, Selmin V, Winzell B. *Progress in Computational Flow–Structure Interaction*. Notes on Numerical Fluid Mechanics and Multidisciplinary Design, vol. 81. Springer: Berlin, 2002.
24. Jameson A. Automatic design of transonic aerofoils to reduce the shock induced pressure drag. *Proceedings of the 31st Israel Annual Conference on Aviation and Aeronautics*, Tel Aviv, 1990; 5–17.
25. Jameson A. Aerodynamic design via control theory. *Journal on Scientific Computing* 1988; **3**:233–260.
26. Reuther J. Aerodynamic shape optimization using control theory. NASA *Technical Report NASA-CR-201064*, 1996.
27. Available from: http://www.optimalsolutions.us/.
28. Samareh JA. Status and future of geometry modeling and grid generation for design and optimization. *Journal of Aircraft* 1999; **36**(1):97–104.
29. Samareh JA. Survey of shape parameterization techniques for high-fidelity multidisciplinary shape optimization. *AIAA Journal* 2001; **39**(5):877–884.
30. Buhmann H. *Radial Basis Functions* (1st edn). Cambridge University Press: Cambridge, 2005.
31. Wendland H. *Scattered Data Approximation* (1st edn). Cambridge University Press: Cambridge, 2005.
32. Rendall TCS, Allen CB. Efficient mesh motion using radial basis functions with data reduction algorithms. *AIAA Paper 2008-305*, *Proceedings of 46th AIAA Aerospace Sciences Meeting*, Reno, January 2008.
33. Vanderplaats GN. *Numerical Optimization Techniques for Engineering Design*: *With Applications*. McGraw-Hill: New York, 1984.
34. Schittkowski K. Test examples for nonlinear programming codes: supplement. *Report*, Institute for Information technology, University of Stuttgart, 1984.
35. Wong WS, Le Moigne A, Qin N. Parallel adjoint-based optimization of a blended wing body aircraft with shock control bumps. *The Aeronautical Journal* 2007; **111**(1117):165–174.




DOI: 10.1002/fld

36. Qin N, Vavalle A, Le Moigne A, Laban M, Huckett K, Weinerfelt P. Aerodynamic studies of blended wing body aircraft. *AIAA-2002-5448*, *The Ninth AIAA/ISSMO Symposium on Multidisciplinary Analysis and Optimization Conference*, September 2002.
37. Qin N, Vavalle A, Le Moigne A. Spanwise lift distribution for blended wing body aircraft. *Journal of Aircraft* 2005; **42**(2):356–365.
38. Wong WS, Qin W, Sellars N, Holden H, Babinsky H. A combined experimental and numerical study of flow structures over three-dimensional shock control bumps. *Aerospace Science and Technology* 2008; **12**(6):436–447.
39. Allen CB. Towards automatic structured multiblock mesh generation using improved transfinite interpolation. *International Journal for Numerical Methods in Engineering* 2008; **74**(5):697–733.
40. Allen CB. Parallel simulation of unsteady hovering rotor wakes. *International Journal for Numerical Methods in Engineering* 2006; **68**(6):632–649.
41. Allen CB. Convergence of steady and unsteady formulations for inviscid hovering rotor solutions. *International Journal for Numerical Methods in Fluids* 2003; **41**(9):931–949.
42. Allen CB. An unsteady multiblock multigrid scheme for lifting forward flight rotor simulation. *International Journal for Numerical Methods in Fluids* 2004; **45**(9):973–984.
43. Allen CB. Parallel universal approach to mesh motion and alication to rotors in forward flight. *International Journal for Numerical Methods in Engineering* 2007; **69**(10):2126–2149.
44. Van-Leer B. *Flux Vector Splitting for the Euler Equations*. Lecture Notes in Physics, vol. 170. Springer: Berlin, 1982; 507–512.
45. Parpia IH. Van-Leer flux vector splitting in moving coordinates. *AIAA Journal* 1988; **26**:113–115.
46. Allen CB. Multigrid convergence of inviscid fixed- and rotary-wing flows. *International Journal for Numerical Methods in Fluids* 2002; **39**(2):121–140.
47. Zingg D, Elias S. Aerodynamic optimization under a range of operating conditions. *AIAA Journal* 2006; **44**(11):2787–2792.
48. Nemec M, Zingg D, Pulliam T. Multipoint and multi-objective aerodynamic shape optimization. *AIAA Journal* 2004; **42**(6):1057–1065.



DOI: 10.1002/fld